Radar-derived bed roughness characterization of Institute and Möller ice streams, West Antarctica, and comparison with Siple Coast ice streams

Robert G. Bingham[1,2] and Martin J. Siegert[3]

Received 26 July 2007; accepted 5 October 2007; published 8 November 2007.

[1] Subglacial bed conditions exert a significant control on ice stream behavior and evolution, and can be characterized by determining bed roughness from FFT analysis of radar-imaged basal reflectors. Here we assess bed roughness across Institute and Möller ice streams, West Antarctica, and compare our findings with bed roughness determined across the Siple Coast ice streams. We find that variations in bed roughness are spatially organized, and attribute this to the varying efficacy of subglacial erosion and deposition, with rougher (inland, slow-flowing) regions largely manifesting preglacial topography, and smoother (downstream, fast-flowing) regions evincing significant postglacial modification to the subglacial landscape. The observed similarities between bed roughness characteristics of IIS/MIS and the Siple ice streams suggest that IIS and MIS are largely underlain by wet, poorly consolidated sediments, and may therefore be vulnerable to the types of dynamical instabilities experienced by the Siple ice streams. **Citation:** Bingham, R. G., and M. J. Siegert (2007), Radar-derived bed roughness characterization of Institute and Möller ice streams, West Antarctica, and comparison with Siple Coast ice streams, *Geophys. Res. Lett.*, *34*, L21504, doi:10.1029/2007GL031483.

1. Introduction

[2] Elucidating the nature of the subglacial interface beneath an ice sheet is critical to determining controls on ice dynamics and the configuration and stability of regions of streaming flow. This is especially pertinent for the West Antarctic Ice Sheet (WAIS), where some ice streams evince both spatial migration and dramatic temporal changes in discharge [*Alley and Bindschadler*, 2001; *Conway et al.*, 2002]. Much of our knowledge of basal conditions beneath the WAIS is derived from studies conducted over the Siple Coast region (Figure 1), where ice streams separated by interstream 'ridges' of slow-flowing ice feed the Ross Ice Shelf. Airborne radio-echo sounding (hereafter RES), seismic analyses, and borehole sampling conducted across this region have revealed that ice streams are underlain extensively by unconsolidated marine sediments, emplaced when the ice sheet was smaller than today. These sediments deform readily when wet facilitating streaming ice flow above despite low driving stresses [*Anandakrishnan et al.*, 1998; *Bell et al.*, 1998; *Tulaczyk et al.*, 2000; *Peters et al.*, 2006].

[3] By contrast, little is known about the flow and basal characteristics of the ice streams that feed the Filchner-Ronne Ice Shelf (FRIS; locations in Figure 1). Institute Ice Stream (IIS; 81.5°S, 75°W) drains one of the largest catchments in the WAIS, disgorging 22.7 ± 2 Gt a^{-1} of mass to the FRIS [*Scambos et al.*, 2004], yet its flow is poorly constrained due to a combination of remoteness and sparse satellite velocity measurements. The existing studies that have discussed ice flow through the region [*Drewry et al.*, 1980; *Scambos et al.*, 2004; *Joughin et al.*, 2006] suggest it may be underlain by weak till, comparable to the Siple ice streams, and therefore the inherent instabilities present in those ice streams might also apply to IIS and flanking regions draining to the FRIS.

[4] Bed roughness, the vertical variation of the subglacial interface with horizontal distance [*Taylor et al.*, 2004], provides a useful first-order summary measure of regional basal characteristics, yielding critical regional-scale insights into ice stream behavior and controls [*Bingham et al.*, 2007; *Siegert et al.*, 2004, 2005]. Here, we calculate bed roughness across IIS and the neighboring Möller Ice Stream (MIS, 82.3S, 65°W) using RES-captured images of the basal reflector. We compare our findings with those from the better known Siple Coast, and use the results to assess the flow, basal characteristics and stability of IIS and MIS, key contributors of the WAIS to the FRIS.

2. Methods

[5] In recent years several approaches have been adopted to characterize bed roughness across parts of Antarctica. One approach is to analyze the detailed surface topographic data now available from satellite altimetry, using transfer functions to invert for variations in basal topography [*Thorsteinsson et al.*, 2003; *Joughin et al.*, 2006]. This method is most effective in regions whose surface velocity fields are well characterized by remote sensing, but 69% of the combined IIS/MIS catchment lies outside current satellite-derived surface velocity fields (Figure 1). Alternative methods utilize bed topography directly imaged by RES. One such approach is to interpolate a two-dimensional basal topographic surface between raw bed returns collected along RES tracks, and calculate the mean and standard deviation of the elevation of each grid cell. Variations in elevation between grid cells can thereon be used to define bed roughness [*Rippin et al.*, 2006]. This method is only viable where RES tracks follow a closely-spaced grid network, which is

[1]British Antarctic Survey, Natural Environment Research Council, Cambridge, UK.
[2]Centre for Polar Observation and Modelling, Bristol Glaciology Centre, School of Geographical Sciences, University of Bristol, Bristol, UK.
[3]Centre for Polar Observation and Modelling, School of GeoSciences, University of Edinburgh, Edinburgh, UK.

0094-8276/07/2007GL031483$05.00

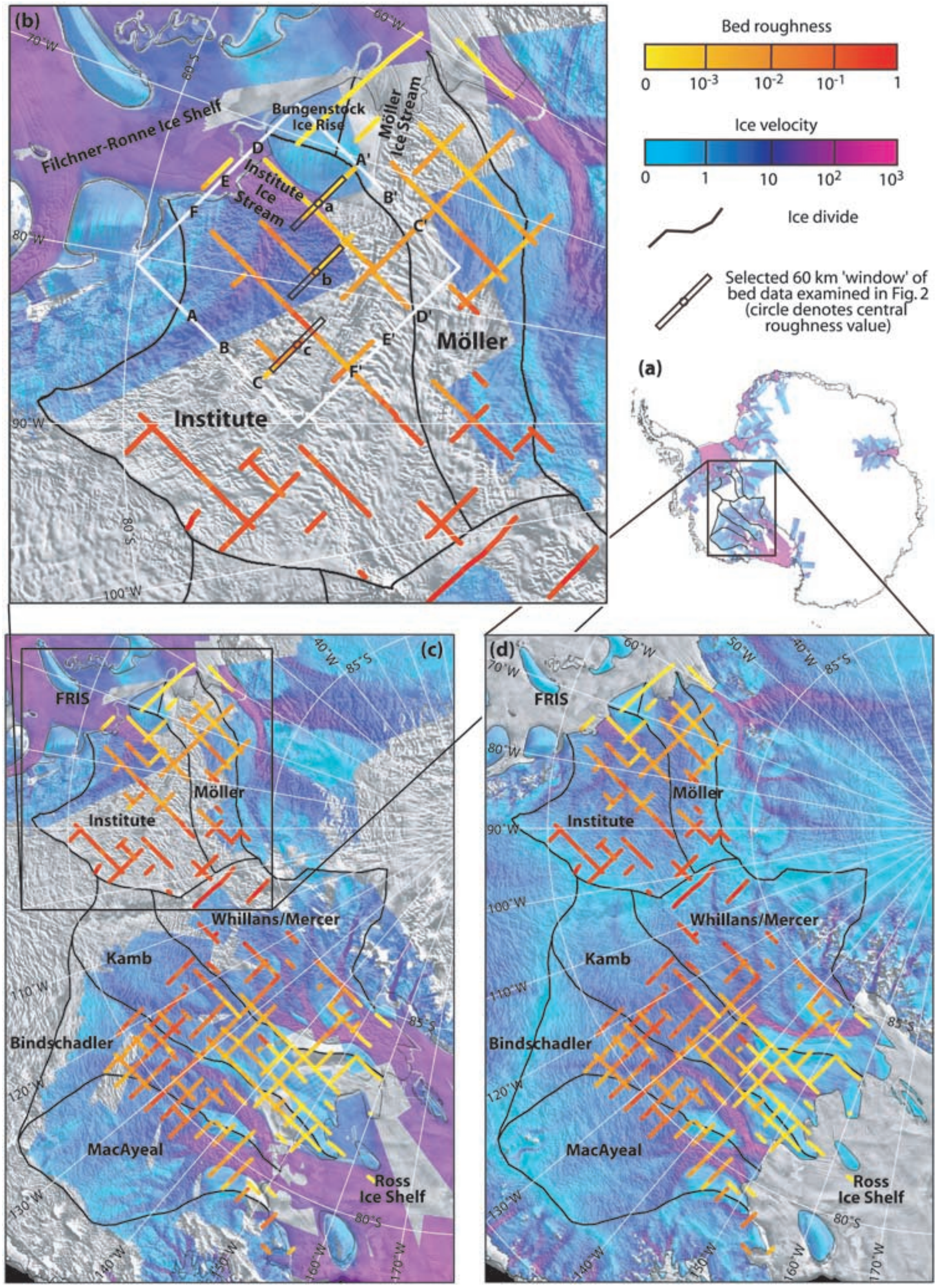

Figure 1. Charts of total bed roughness along RES lines for catchments draining to the Filchner-Ronne (FRIS) and Ross Ice Shelves. (a) Catchment locations superimposed over surface ice velocities [after *Joughin et al.*, 2006; *Rignot*, 2006]. Along-RES-track bed roughness superimposed over MOA imagery [*Haran et al.*, 2006], over which is draped either the (b) and (c) available coverage of satellite-derived surface ice velocities or (d) depth-averaged balance velocities [after *Le Brocq et al.*, 2006]. In Figure 1b, a, b, and c mark selected elevation profiles analyzed for bed roughness power spectra in Figure S1. The white boxed area and upper-case letters locate bed roughness profiles analyzed in Figure S2.

not the case for the available data over IIS and MIS (Figure 1). The remaining alternative is to interrogate RES data directly along-track to extract the spectral roughness of subglacial topography [*Taylor et al.*, 2004; *Siegert et al.*, 2004, 2005; *Bingham et al.*, 2007]. To date, limited satellite coverage and the remoteness of the IIS/MIS region have deferred an analysis of its basal properties, yet bed returns are available from a wide-ranging airborne RES survey conducted across the region between 1977 and 1979. Here we calculate bed roughness directly along these RES flight tracks spanning IIS and MIS.

[6] The RES data analyzed here were obtained by the Scott Polar Research Institute/National Science Foundation/Technical University of Denmark (SPRI-NSF-TUD) consortium between 1977 and 1979. Details of the surveys, including navigation and errors, are provided in the auxil-

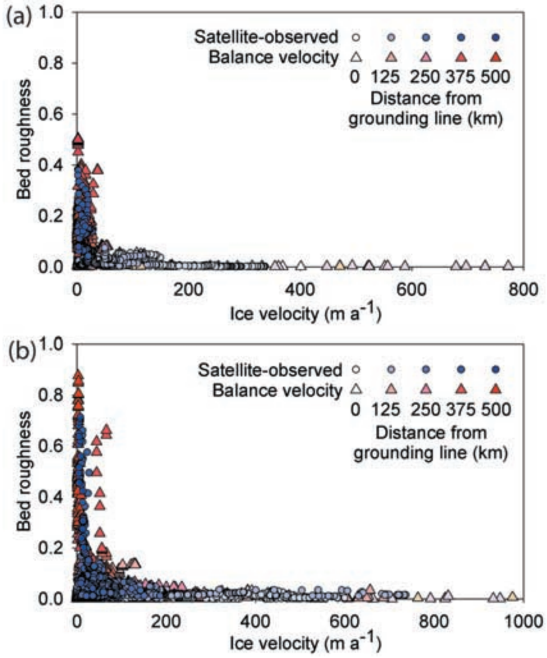

Figure 2. Dimensionless bed roughness values calculated along RES lines in Figure 1 compared with satellite-observed ice velocities (as mapped in Figure 1c) and depth-averaged balance velocities (as mapped in Figure 1d) across the (a) Institute and Möller and (b) Siple Coast catchments (Whillans/Mercer, Kamb, Bindschadler, and MacAyeal as delineated in Figures 1c and 1d). The symbols are shaded such that darker symbols are close to the grounding line and lighter symbols are far from the grounding line.

iary materials [see also *Drewry*, 1983; *Siegert*, 1999].[1] Critically, they comprise the only RES data ever collected over the remote IIS and MIS, and as such provide the only data that can be used directly to characterize their basal properties. The quality of the SPRI-NSF-TUD data has been compared favorably elsewhere in Antarctica with modern datasets [*Siegert et al.*, 2004; *Bingham et al.*, 2007]. Over 7000 km of flight track are available over the IIS/MIS region; the bed is imaged in 72% of 4117 shots analyzed.

[7] The roughness of the basal reflector was calculated using a Fast Fourier-Transform- (FFT-) based technique, which characterizes the wavelength-related vertical variation of a surface with horizontal distance [*Taylor et al.*, 2004]. Each FFT was applied over a moving 60-km window, bed roughness being the integral of the resulting FFT spectral power density plot for each analysis window (for examples and further information, see auxiliary materials, section S2). Each bed roughness value is plotted at the centrepoint of its analysis window, providing a spatial map of bed roughness variations along flight tracks over the WAIS (Figure 1). We compare the roughness variations with satellite-derived ice-surface velocities [after *Joughin et al.*, 2006] and depth-averaged balance velocities [after *Le Brocq et al.*, 2006]. We consider both of these velocity datasets because the satellite-derived data cover only 31% of the IIS/MIS region (Figure 1b), thus balance velocities can be used as proxies for ice flow elsewhere.

3. Results

[8] Across the Institute and Möller catchments total bed roughness ranges between 0.0002 and 0.504, averaging 0.057, comparable to values measured across the Siple Coast [*Siegert et al.*, 2004]. The roughness values exhibit clear spatial organization (Figure 1). Beneath the main trunk of IIS the basal reflector is remarkably smooth, never rising above 0.01 between points D and a on Figure 1b. Beneath the downstream portion of MIS too, the basal reflector is relatively smooth, remaining below 0.03 downstream of point C' (Figure 1b). Away from the regions of active streaming, and with distance from the grounding line towards the ice divides, the basal reflector becomes progressively rougher. These findings are true regardless of whether the roughness windows analyzed are quasi-parallel or quasi-orthogonal to ice flow, and mirror spatial variations in bed roughness found across the Siple Coast (see Figures 1c and 1d). Further support for this statement is given in auxiliary materials, section S3.

[9] In Figure 2, bed roughness is plotted versus ice velocity. Only very low bed roughness values are attained where ice speeds are high, whereas high bed roughness is only measured where ice speeds are low (Figure 2a). Typically, away from the grounding line, where ice flows more slowly, bed roughness is high. Towards the grounding line, where ice velocities are more variable but can be very high, bed roughness is low (Figure 2a).

[10] Plotting roughness values directly against distance from the grounding line (Figure 3) reveals the ice stream beds become progressively smoother towards the grounding line, such that $y = ae^{bx}$, where y = bed roughness (dimensionless), a and b are constants that vary between individual catchments, and x = distance from the grounding line (km; derivation outlined in auxiliary materials, section S4). For both IIS and MIS the coefficient of determination (R^2) for this relation is >0.5, thus >50% of the variation in roughness is 'explained' by the distance of the roughness datapoint from the grounding line. Conducting the same exercise for the four Siple catchments delineated in Figure 1c confirms that the same relation also applies strongly over the Whillans/Mercer and Kamb catchments (Figures 3c and 3d), and is especially strong for the Kamb catchment, yielding an R^2 of 0.77. The same relationship is weaker over the Bindschadler and MacAyeal catchments ($R^2 < 0.5$), probably in the latter case due to insufficient data coverage in upstream parts of the catchment (Figures 3e and 3f).

4. Discussion

[11] Our results demonstrate bed roughness varies in a distinct spatially-organised manner beneath the two largest catchments feeding the FRIS. The roughness trends provide unique insights into the subglacial environment across this poorly known region. The parallel with the general pattern of roughness variations observed across the Siple Coast region is striking, and suggests strongly that the subglacial environments beneath the two regions are analogous. Beneath the Siple Coast ice streams smooth basal reflectors

[1] Auxiliary material data sets are available at ftp://ftp.agu.org/apend/gl/2007gl031483. Other auxiliary material files are in the HTML.

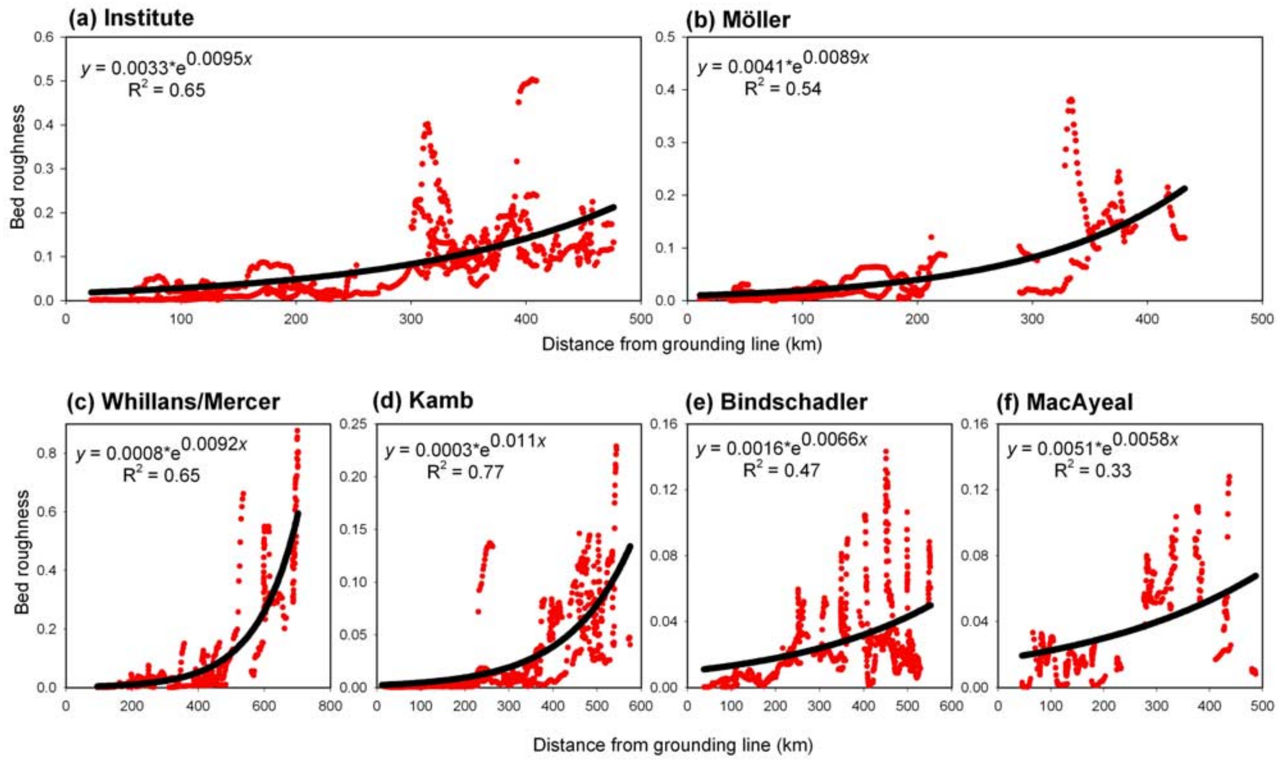

Figure 3. Plots of bed roughness versus distance from the grounding line for (a)–(b) the Institute and Möller catchments and (c)–(f) the Siple catchments.

have been linked to the subglacial existence of unconsolidated sediments that deform readily when wet, allowing fast flow to persist despite low driving stresses [*Engelhardt and Kamb*, 1998; *Tulaczyk et al.*, 2000; *Blankenship et al.*, 2001; *Peters et al.*, 2006]. IIS also exhibits fast flow and low driving stresses [*Scambos et al.*, 2004; *Joughin et al.*, 2006] together with a smooth basal reflector (Figure 1a). Hence the most likely explanation for this combination of phenomena is a widespread unconsolidated sediment layer beneath IIS and much of its catchment. There is no increase in bed roughness moving eastwards from the lower 200 km of IIS across the slow-flowing Bungenstock Ice Rise and into the downstream 200 km of MIS (Figure 1a; see also plot AA′ in Figure S2), and this likely reflects a thick basal sediment layer pervading most of the IIS/MIS region fringing the FRIS.

[12] Subglacial roughness properties beneath the IIS and MIS catchments are most analogous to those beneath the Kamb and Whillans/Mercer catchments. All four catchments are characterised by a distinct roughening of subglacial topography with distance inland (Figure 3) and with downstream beds uniformly smooth regardless of whether they underlie contemporary ice streams or interstream ridges. The similarity is significant, because the Kamb Ice Stream is demonstrably prone to unstable behaviour, presenting evidence of several earlier periods of fast flow and lateral migration preceding its current stagnant state [*Retzlaff and Bentley*, 1993; *Bentley et al.*, 1998; *Kamb*, 2001; *Catania et al.*, 2003]. A recent slowdown of Whillans Ice Stream suggests it too is prone to similar dynamic behaviour [*Bougamont et al.*, 2003]. Key to the inherent instability of the Kamb and Whillans ice streams is thought to be a thick underlying deformable sediment layer and an absence of constraining subglacial topography [*Kamb*, 2001; *Bougamont et al.*, 2003; *Siegert et al.*, 2004]. The ubiquity of the sediments tends to dampen subglacial topographic protuberances, leaving few constraints to lateral migrations of the ice streams; much of the unstable behaviour has instead been linked to fluctuating thermal conditions in the sediments which deform readily when wet but stiffen when frozen [*Tulaczyk et al.*, 2000]. The inference that a thick swathe of deformable basal sediments also underlies IIS and MIS suggests therefore that these two FRIS ice streams are likely vulnerable to similar dynamic instabilities.

[13] Boreholing to the beds of Whillans, Kamb and Bindschadler ice streams and their interstream ridges has revealed the subglacial tills beneath the region are primarily composed of Tertiary marine sediments [*Engelhardt et al.*, 1990; *Engelhardt and Kamb*, 1998; *Kamb*, 2001]. Aerogeophysical surveying has been used to assess the likely distribution of the sediments over the Siple Coast region by isostatically adjusting the subglacial topography to demarcate the paleo-shoreline, below which marine sedimentation would have been possible prior to the formation of the WAIS and/or during periods of ice-sheet collapse [*Studinger et al.*, 2001]. The areas with the most sediment correspond with smooth basal reflectors, suggesting ‘smoothness’ can be used elsewhere as an indicator of subglacial marine sediments. A physical explanation is provided by considering rougher beds as legacies of a mountainous preglacial landscape, and smoother beds as symptomatic of its progressive burial beneath marine sediments. We therefore interpret the widespread region of smooth subglacial topography underlying the lower sectors of IIS and MIS as an

extensive covering of marine sediments emplaced when the ice-sheet was less advanced than today.

[14] The existence of such a smooth deforming basal sediment layer would offer no basal constraint to previous or future lateral migrations of IIS and MIS, and does not discount the possibility that they may be subject to periods of stagnation. The possibility of such unstable behavior has implications for the history and future stability of the FRIS, to which these ice streams, especially IIS, are significant contributors. We therefore support the contention of *Scambos et al.* [2004] that sampling of basal sediments beneath IIS would offer valuable scientific insights. If the basal material is marine, and was therefore emplaced when the ice sheet was smaller than today, it could be dated to constrain when the region was last glaciated, providing critical insights into the age and stability of the FRIS and the WAIS.

5. Conclusions

[15] Applying FFT analysis to airborne radar data collected over Institute Ice Stream (IIS) and Möller Ice Stream (MIS), West Antarctica, we have determined spatial variations in the roughness of the bed that correspond with variations in ice flow and distance from the grounding line. Typically, the bed is smoother where ice flows faster and towards the grounding line, whereas the bed is rougher where ice flows more slowly and towards the ice divides. The variations in bed roughness most likely reflect differences in the efficacy of erosion and deposition beneath the ice. They mirror similar variations beneath the Siple Coast ice streams, and are most similar to bed roughness characteristics across the Kamb and Whillans/Mercer catchments. Across the downstream sectors of IIS and MIS and the intervening Bungenstock Ice Rise the basal reflector is contiguously smooth. By analogy with earlier Siple Coast-based studies, we contend that IIS and MIS are widely underlain by unconsolidated marine sediments, and therefore these key contributors to the Filchner-Ronne Ice Shelf may be vulnerable to the types of dynamical instabilities experienced by the Siple Coast ice streams.

[16] **Acknowledgments.** This work was conducted in and supported by the NERC Centre for Polar Observation and Modelling. We thank two anonymous reviewers and the scientific editor E. Rignot for their useful critical insights on an earlier version of the manuscript.

References

Alley, R. B., and R. A. Bindschadler (Eds.) (2001), *The West Antarctic Ice Sheet: Behavior and Environment*, *Antarct. Res. Ser.*, vol. 77, AGU, Washington, D. C.

Anandakrishnan, S., D. D. Blankenship, R. B. Alley, and P. L. Stoffa (1998), Influence of subglacial geology on the position of a West Antarctic ice stream from seismic observations, *Nature*, *394*, 62–65, doi:10.1038/27889.

Bell, R. E., et al. (1998), Influence of subglacial geology on the onset of a West Antarctic ice stream from aerogeophysical observations, *Nature*, *394*, 58–62, doi:10.1038/27883.

Bentley, C. R., N. Lord, and C. Liu (1998), Radar reflections reveal a wet bed beneath stagnant Ice Stream C and a frozen bed beneath ridge BC, West Antarctica, *J. Glaciol.*, *44*, 149–156.

Bingham, R. G., M. J. Siegert, D. A. Young, and D. D. Blankenship (2007), Organized flow from the South Pole to the Filchner-Ronne Ice Shelf: An assessment of balance velocities in interior East Antarctica using radio-echo sounding data, *J. Geophys. Res.*, *112*, F03S26, doi:10.1029/2006JF000556.

Blankenship, D. D., et al. (2001), Geological controls on the initiation of rapid basal motion for West Antarctic ice streams: A geophysical perspective including new airborne radar sounding and laser altimetry results, in *The West Antarctic Ice Sheet: Behavior and Environment*, *Antarct. Res. Ser.*, vol. 77, edited by R. B. Alley and R. A. Bindschadler, pp. 105–121, AGU, Washington, D. C.

Bougamont, M., S. Tulaczyk, and I. Joughin (2003), Numerical investigations of the slowdown of Whillans Ice Stream, West Antarctica: Is it shutting down like Ice Stream C?, *Ann. Glaciol.*, *36*, 239–246.

Catania, G. A., H. B. Conway, A. M. Gades, C. F. Raymond, and H. Engelhardt (2003), Bed reflectivity beneath inactive ice streams in West Antarctica, *Ann. Glaciol.*, *36*, 287–291.

Conway, H., G. Catania, C. F. Raymond, A. M. Gades, T. M. Scambos, and H. Engelhardt (2002), Switch of flow direction in an Antarctic ice stream, *Nature*, *419*, 465–467, doi:10.1038/nature01081.

Drewry, D. J. (Ed.) (1983), *Antarctica: Glaciological and Geophysical Folio*, Cambridge Univ. Press, Cambridge, UK.

Drewry, D. J., D. T. Meldrum, and E. Jankowski (1980), Radio echo and magnetic sounding of the Antarctic Ice Sheet, 1978–79, *Polar Rec.*, *20*, 43–57.

Engelhardt, H., and B. Kamb (1998), Basal sliding of Ice Stream B, West Antarctica, *J. Glaciol.*, *44*, 223–230.

Engelhardt, H., N. Humphrey, B. Kamb, and M. Fahnestock (1990), Physical conditions at the base of a fast moving Antarctic ice stream, *Science*, *248*, 57–59.

Haran, T., J. Bohlander, T. Scambos, and M. Fahnestock (2006), MODIS Mosaic of Antarctica (MOA) Image Map, http://nsidc.org/data/nsidc-0280.html, Natl. Snow and Ice Data Cent., Boulder, Colo.

Joughin, I., J. L. Bamber, T. Scambos, S. Tulaczyk, M. Fahnestock, and D. R. MacAyeal (2006), Integrating satellite observations with modelling: Basal shear stress of the Filchner-Ronne ice streams, Antarctica, *Philos. Trans. R. Soc., Ser. A*, *364*, 1795–1814, doi:10.1098/rsta.2006.1799.

Kamb, B. (2001), Basal zone of the West Antarctic ice streams and its role in lubrication of their rapid motion, in *The West Antarctic Ice Sheet: Behavior and Environment*, *Antarct. Res. Ser.*, vol. 77, edited by R. B. Alley and R. A. Bindschadler, pp. 157–199, AGU, Washington, D. C.

Le Brocq, A. M., A. J. Payne, and M. J. Siegert (2006), West Antarctic balance calculations: Impact of flux-routing algorithm, smoothing and topography, *Comput. Geosci.*, *32*, 1780–1795, doi:10.1016/j.cageo.2006.05.003.

Peters, L. E., S. Anandakrishnan, R. B. Alley, J. P. Winberry, D. E. Voigt, A. M. Smith, and D. L. Morse (2006), Subglacial sediments as a control on the onset and location of two Siple Coast ice streams, West Antarctica, *J. Geophys. Res.*, *111*, B01302, doi:10.1029/2005JB003766.

Retzlaff, R., and C. R. Bentley (1993), Timing of stagnation of Ice Stream C, West Antarctica, from short-pulse radar studies of buried surface crevasses, *J. Glaciol.*, *39*, 553–561.

Rignot, E. (2006), Changes in ice dynamics and mass balance of the Antarctic ice sheet, *Philos. Trans. R. Soc., Ser. A*, *364*, 1637–1656, doi:10.1098/rsta.2006.1793.

Rippin, D. M., J. L. Bamber, M. J. Siegert, D. G. Vaughan, and H. F. J. Corr (2006), Basal conditions beneath enhanced-flow tributaries of Slessor Glacier, East Antarctica, *J. Glaciol.*, *52*, 481–490.

Scambos, T., J. Bohlander, B. Raup, and T. Haran (2004), Glaciological characteristics of Institute Ice Stream using remote sensing, *Antarctic Sci.*, *16*, 205–213, doi:10.1017/S0954102004001919.

Siegert, M. J. (1999), On the origin, nature and uses of Antarctic ice-sheet radio-echo layering, *Prog. Phys. Geogr.*, *23*, 159–179.

Siegert, M. J., J. Taylor, A. J. Payne, and B. Hubbard (2004), Macro-scale bed roughness of the Siple Coast ice streams in West Antarctica, *Earth Surf. Processes Landforms*, *29*, 1591–1596, doi:10.1002/esp.1100.

Siegert, M. J., J. Taylor, and A. J. Payne (2005), Spectral roughness of subglacial topography and implications for former ice-sheet dynamics in East Antarctica, *Global Planet. Change*, *45*, 249–263, doi:10.1016/j.gloplacha.2004.09.008.

Studinger, M., R. E. Bell, D. D. Blankenship, C. A. Finn, R. A. Arko, D. L. Morse, and I. Joughin (2001), Subglacial sediments: A regional geological template for ice flow in West Antarctica, *Geophys. Res. Lett.*, *28*, 3493–3496.

Taylor, J., M. J. Siegert, A. J. Payne, and B. Hubbard (2004), Regional-scale bed roughness beneath ice masses: Measurement and analysis, *Comput. Geosci.*, *30*, 899–908, doi:10.1016/j.cageo.2004.06.007.

Thorsteinsson, T., et al. (2003), Bed topography and lubrication inferred from surface measurements on fast-flowing ice streams, *J. Glaciol.*, *49*, 481–490.

Tulaczyk, S., W. B. Kamb, and H. F. Engelhardt (2000), Basal mechanics of ice stream B, West Antarctica: 1. Till mechanics, *J. Geophys. Res.*, *105*, 463–481.

R. G. Bingham, British Antarctic Survey, Natural Environment Research Council, High Cross, Madingley Road, Cambridge CB3 0ET, UK. (rgbi@bas.ac.uk)

M. J. Siegert, Centre for Polar Observation and Modelling, School of GeoSciences, University of Edinburgh, Grant Institute, The King's Buildings, West Mains Road, Edinburgh EH9 3JW, UK.

Auxiliary material for Paper 2007gl031483

Radar-derived bed roughness characterization of Institute and Möller ice streams, West Antarctica, and comparison with Siple Coast ice streams

Robert G. Bingham
British Antarctic Survey, Natural Environment Research Council, Cambridge, U. K.

Centre for Polar Observation and Modelling, Bristol Glaciology Centre, School of Geographical Sciences, University of Bristol, Bristol, U. K.

Martin J. Siegert
Centre for Polar Observation and Modelling, School of GeoSciences, University of Edinburgh, Edinburgh, U. K.

Bingham, R. G., and M. J. Siegert (2007), Radar-derived bed roughness characterization of Institute and Möller ice streams, West Antarctica, and comparison with Siple Coast ice streams, Geophys. Res. Lett., 34, L21504, doi:10.1029/2007GL031483.

Introduction

The auxiliary data provided here come in the form of a text document containing four sections describing, in turn, (1) RES data acquisition, (2) roughness calculations, (3) bed roughness
profiles across and along IIS, and (4) distance to the grounding line. Section 2 makes reference to Figure S1. Section 3 makes reference to Figure S2. Section 4 makes reference to Table S1.

1. 2007gl031483-ts01.txt
Details of the derivation of X, the (x, y) coordinates of peak ice flow over the grounding line, for six West Antarctic catchments.
1.1 Column "Catchment", no units, contains two subsections, "Ronne catchments" contains "Institute" and "Möller", "Ross catchments" contains "Whillans/Mercer", "Kamb", "Bindschadler" and "MacAyeal".
1.2 Column "Derivation of X", no units, text description of method used to define position of X, the xy coordinates of fastest flow over the grounding line for a given catchment.
1.3 Column "Coordinates of X", latitude & longitude position of X for a given catchment
1.4 Column "Satellite-derived ice surface velocity at X", units m a-1 (metres per year)
1.5 Column "Balance velocity at X", units m a-1 (metres per year)

2. 2007gl031483-fs01.tif
Examples of bed roughness power spectra for selected 60 km ‘windows’ of continuous RES bed returns within the Institute catchment (locations in Fig. 1b). (a) Elevation profiles used to calculate power spectra. (b) Bed roughness (FFT) power spectra for the elevation profiles in (a). Total bed roughness, plotted in Fig. 1 at the centrepoint of the profile, is calculated as the integral of the normalized power spectra. In this example, total bed roughness increases from profile a through to c, as we move away from the grounding line towards the ice divide.

3. 2007gl031483-fs02.tif
Profiles of bed elevation, bed roughness and ice velocity across (a) 3 parallel lines trending WNW-ESE and (b) 3 parallel lines trending NNE-SSW across the Institute Ice Stream catchment. In each chart, bed elevation (thin black line) is plotted on the lower tier; and bed roughness (thick black line, left axis), satellite-derived ice velocity (thin black line, right axis) and balance velocity (thin gray line, right axis) are plotted on the upper tier. Profile locations are shown in Fig. 1b.

Radar-derived bed roughness characterization of Institute and Möller ice streams, West Antarctica, and comparison with Siple Coast ice streams

R. G. Bingham and M. J. Siegert

S1. RES data acquisition

The RES data used in the analysis were derived from the extensive Scott Polar Research Institute/National Science Foundation/Technicial University of Denmark (SPRI-NSF-TUD) airborne surveys conducted over the Antarctic Ice Sheet between 1977 and 1979. Collected with a 250 ns 60 MHz pulse RES system, bed returns were recorded to file at 20 s intervals using a semi-automatic trace reader, and were subsequently corrected and tied to navigation records obtained by an aerogeophysical inertial system. This yielded bed elevations with an average along-track sampling resolution of 1.85 km, with errors in absolute position < 5 km (typically 1 km), and errors in sampling interval at least two orders of magnitude lower. Vertical errors are of the order of ñ 25 m, resulting from a combination of digitizing errors, velocity corrections, and corrections to aircraft altitude measurements. Although modern RES methods routinely achieve greater precision and navigational accuracy, these errors are sufficiently low not to affect detrimentally our regional-scale bed roughness analysis. Significantly, these RES data are the only such data ever collected over the remote Institute and M”ller Ice Stream catchments, and as such constitute our only means of analysing directly their basal properties. Over 7000 km of flight track are available over the region; the bed is imaged in 72% of 4117 shots analysed.

S2. Roughness calculations

Bed roughness was calculated point-by-point along RES flightlines using the forward Fast Fourier Transform (FFT) routine available in the software package Microcal Origin 5.0. Preconditions for the FFT are the use of 2N datapoints, and a suggested minimum value of N = 5 gives lines 32 datapoints long. With this dataset's mean sampling resolution of 1.85 km, this gives a minimum FFT window length of 60 km. Each 32-datapoint window was detrended linearly using least-squares regression, to eliminate the dominance of very long wavelength (> 30 km, i.e., half the window length) roughness, and amplitude was normalised with respect to N. Bed roughness (plotted in Figure 1 at the centrepoint of each 32-datapoint analysis window) is defined
as the integral of the resulting FFT spectral power density plot for each analysis window. Some examples of the roughness power spectra plots for profiles of varying bed roughness (locations shown in Figure 1b) are provided in Figure S1.

S3. Bed roughness profiles across and along IIS

In Figure S2, we present, for 3 parallel profiles trending WNW-ESE (AA', BB' and CC') and 3 parallel profiles trending NNE-SSW (DD', EE' and FF') across the downstream sector of the Institute catchment, plots of bed elevation and bed roughness together with ice velocities derived from satellite data and balance-flux modeling. Moving progressively away from the grounding line and towards the ice-sheet interior (i.e. from AA' through BB' to CC'), mean bed roughness generally increases, in tandem with a fall in ice flow velocity. Moving progressively WNW away from the main trunk of IIS (i.e. from DD' through EE' to FF'), mean bed roughness again increases as ice velocities decrease. These trends are confirmed by analyzing profiles AA' and DD' individually. From A to A' we travel downstream along a western tributary to IIS, gradually approaching and ultimately crossing the IIS trunk to the Bungenstock Ice Rise (Figure 1b); as we do so, bed roughness decreases and ice velocities increase until the IIS/Bungenstock boundary is traversed. Profile DD' heads upstream along the main trunk of IIS (Figure 1b), and again highlights increasing bed roughness corresponding with falling ice velocities with distance from the grounding line.

S4. Distance to the grounding line

The distance of a given bed roughness datapoint from the grounding line, x, was calculated as follows. For each of the 6 ice stream catchments analysed in this study, we defined a point X(x,y) at which ice flow over the grounding line is at a peak. Where possible, this was calculated directly from satellite data, but for the M”ller, Kamb, Bindschadler and MacAyeal catchments satellite determination of ice velocities over the grounding line is incomplete, requiring the use of alternative proxies as given in Table S1. The distance to the grounding line of any given roughness datapoint was calculated as the straight-line distance between the roughness datapoint and X for the catchment in which the roughness point is located.

Catchment	Derivation of X	Coordinates of X	Satellite-derived ice surface velocity at X (m a-1)	Balance velocity at X (m a-1)
Ronne catchments				
Institute	Peak velocity across grounding line determined directly from Rignot [2006].	80.93 °S, 73.34 °W	395.8	203.8
M”ller	Peak balance velocity [Le Brocq et al., 2006] across coastline from Antarctic Digital Database.	82.33 °S, 66.31 °W	Unavailable	151.3
Ross catchments				
Whillans/Mercer	Peak velocity across grounding line determined directly from Rignot [2006].	84.21 °S, 164.21 °W	417.7	Unavailable
Kamb	Point of peak flow across 'grounding line' determined by comparing Rignot [2006] with Le Brocq et al. (2006) across coastline from Antarctic Digital Database.	82.57 °S, 152.75 °W	< 10	828.5
Bindschadler	Point of peak flow across 'grounding line' determined by comparing Rignot [2006] with Le Brocq et al. (2006) across coastline from Antarctic Digital Database.	80.67 °S, 149.81 °W	460.6	331.2
MacAyeal	Point of peak flow across 'grounding line' determined by comparing Rignot [2006] with Le Brocq et al. (2006) across coastline from Antarctic Digital Database.	79.98 °S, 149.99 °W	484.4	86.8

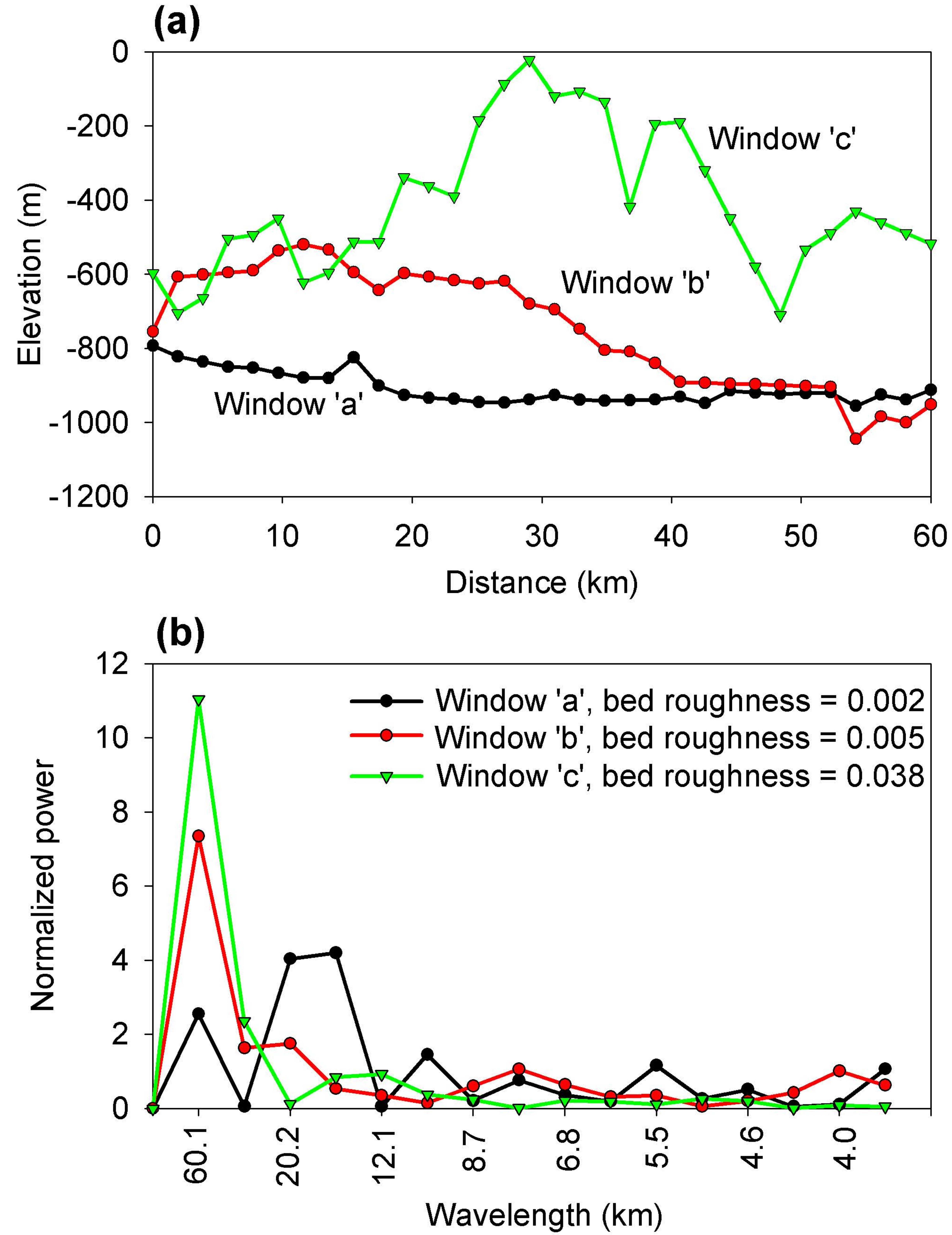
(a)
Elevation (m)
0
-200
-400
-600
-800
-1000
-1200
Window 'c'
Window 'b'
Window 'a'
0
10
20
30
40
50
60
Distance (km)
(b)
Normalized power
12
10
8
6
4
2
0
Window 'a', bed roughness = 0.002
Window 'b', bed roughness = 0.005
Window 'c', bed roughness = 0.038
60.1
20.2
12.1
8.7
6.8
5.5
4.6
4.0
Wavelength (km)


(a) Profiles trending WNW - ESE
Bed roughness
Bedrock elevation (m)
Ice velocity (m a-1)
A
A'
B
B'
C
C'
Distance along profile (km)
(b) Profiles trending NNE - SSW
D
D'
E
E'
F
F'
Legend for upper tiers:
Bed roughness (left-hand scale)
Satellite-derived surface velocity (right-hand scale)
Depth-averaged balance velocity (right-hand scale)